pISSN 1598-298X / eISSN 2384-0749
J Vet Clin 37(1) : 28-33 (2020)
http://dx.doi.org/10.17555/jvc.2020.02.37.1.28

Journal of Veterinary Clinics
www.ksvc.or.kr

Quantitative Assessment of Salivary Gland washout in Clinically Healthy Dogs

Won-seok Jang, Tae-sung Hwang, Dong-in Jung, Jae-hoon Lee and Hee-chun Lee[1]

Institute of Animal Medicine, College of Veterinary Medicine, Gyeongsang National University, Jinju 52828, Korea

(Received: September 01, 2019 / Accepted: February 12, 2020)

Abstract : The aims of this study were to obtain the normal ranges of enhancement parameters for salivary gland in dynamic CT and to investigate the effects of fasting time on contrast enhancement in clinically normal beagle dogs. With five healthy beagle dogs, dynamic CT examination was performed according to fasting times (as fasting times, 12 hours, 0 min, 20 min, 40 min, 1 hours, 6 hours, 24 hours). In normal beagles with 12 hours fasting, enhancement parameters through the preliminary study were as follows: ImaxA – 472.49 ± 19.01 HU; ImaxS – 138.95 ± 6.25 HU; TmaxA – 25.8 ± 1.79 sec; TmaxS – 69.0 ± 23.11 sec; Teq – 80.5 ± 6.61 sec; T-Aeq – 54.5 ± 5.51 sec (Imax – peak enhancement; Tmax – time to peak enhancement; Teq – time to equilibrium phase; T-Aeq – time between peak enhancement in the common carotid artery and onset of the equilibrium phase; A – common carotid; S – submandibular gland; HU – Hounsfield unit). Additionally, ImaxA and ImaxS were significantly increased in 40 min after eating. Because these results associated with postprandial hemodynamic changes can make the diagnosis of salivary gland diseases more difficult, sufficient fasting time is important for accurate diagnosis.

Key words **:** contrast enhancement, dogs, dynamic computed tomography, enhancement parameters, salivary gland.

Introduction

Contrast-enhanced computed tomography (CECT) is used to enhance the contrast between pathologic, normal organ structures, and surrounding tissues to find lesions. CECT is routinely performed in humans (2,3,30) as well as in the in the veterinary field (9,12,31). To establish optimal imaging conditions for CECT, dynamic computed tomography (CT) should be performed prior to CECT (5,20,36).

In human medicine, differentiating between various salivary gland diseases or between tumor types has been studied using dynamic CT (8,23,37,39). Computed tomographic features of salivary gland diseases such as sialolithiasis, mucocele, sialadenitis and adenocarcinoma have been studied in veterinary medicine (6,7,21,22,35). However, there are no studies, in which dynamic CT was applied to the lesions in the salivary glands. The protocol to obtain optimal scanning time for salivary gland has not, also, been established. Therefore, it is expected that establishing normal reference ranges for dynamic CT enhancement parameters of salivary gland will enhance the usefulness of CT in diagnosing salivary gland diseases.

The aims of this study were to obtain the reference ranges, as preliminary experimentation, for dynamic CT of salivary gland in clinically normal dogs and to evaluate whether the postprandial hemodynamic changes have effects on contrast enhancement.

[1]Corresponding author.
E-mail : lhc@gnu.ac.kr

Materials and Methods

Preparation and general anesthesia of experimental animals

All procedures were approved by the Institutional Animal Care and Use Committee at Gyeongsang National University and the dogs were cared for according to the Guidelines for Animal Experiments (GNU-170227-D0006) of Gyeongsang National University. Five healthy beagle dogs (mean weight 10.6 kg, range 8.7-12.1; mean age 4 years; five males) were used in a crossover method and the experiments were performed. Using physical examination and abdominal radiographs, they were screened for evidence of gastrointestinal disease. The minimum time delay between consecutive examinations in the same dog was 2 weeks to allow complete renal excretion of the contrast medium.

In this study, seven groups with varying fasting times (As fasting times, 12 hours, 0 min, 20 min, 40 min, 1 hour, 6 hours, and 24 hours) before dynamic CT examination were applied to the five healthy dogs. 12H group (12 hours fasting time before dynamic CT examination) was set to represent the protocol in general use in small animal clinics (14).

During fasting, care was taken that the animals did not have any visual and olfactory contact with the test meal to be fed later. The test meal consisted of daily ration of dry dog food (Original Ultra.®, Natural Balance Korea. Co., Ltd., Gyeonggi-Do, Korea).

All dogs were premedicated with glycopyrrolate (0.01 mg/kg, SC, Mobinulinj.®, Myungmoon pharm. Co., Ltd., Seoul, Korea). Anesthesia was induced with alfaxalone (2 mg/kg, IV, Alfaxan inj.®, Careside. Co., Ltd., Gyeonggi-Do, Korea;

6 mg/kg IV) through a 22-gauge intravenous catheter and 3-way stopcock in the right cephalic vein. General anesthesia was maintained with isoflurane (Ifran®, Hana pharm. Co., Ltd., Kyonggi-Do, Korea) in oxygen (2 L/min) via endotracheal (ET) intubation. All dogs were intubated with ET-tube and position was ventral recumbency.

Injection protocols of contrast medium

The present study used non-ionic contrast medium Iohexol (Omnipaque 300®, GE Healthcare Ireland) containing 300 mg I/ml. The contrast medium was administered by the use of an automated power injector (CT 9000^{TM} ADV injector, Mallinckrodt, Germany) with a 22-gauge intravenous catheter and 3-way stopcock into the cephalic vein. A 2 ml/kg intravenous bolus of contrast agent was injected at 1 ml/s.

Protocols of dynamic CT

The examinations were performed on a two-channel multidetector helical CT scanner (Somatom Emotion®, SIEMENS Medical Systems, Erlangen, Germany). Thirty-five dynamic CT scans were obtained with dogs positioned in dorsal recumbency under general anesthesia and a total seven single-level dynamic CT examinations per dog with seven groups of fasting times were performed in five beagle dogs.

Dynamic CT was evaluated at the region of submandibular gland, as the biggest salivary gland, including common carotid artery. In dogs, submandibular gland is commonly located caudally to the mandibular ramus (6). In all examinations, a topogram was initially performed to establish the region of where mandibular ramus is located. Pre-contrast images from the mandibular ramus to 2nd cervical spine, including submandibular gland and common carotid artery, were obtained. One of the pre-contrast images was determined as a single level which visualize the submandibular gland and common carotid artery concurrently. The selection of a level was followed by single-level, contrast-enhanced dynamic CT study after a contrast medium administration.

The scanning parameters of the dynamic CT were as follows: Peak kilovoltage 110 kVp, tube current 50 mAs, 1 sec rotation time, 2 sec intervals, and slice thickness 5.0 mm. The time delay between the beginning of the contrast medium injection and the start of scanning was 3 sec for each examination and 50 images were obtained every 2 sec for 100 sec.

Image analysis

All dynamic CT images were analyzed at a workstation with OsiriX (Pixmeo, Geneva, Switzerland), which is a clinically used PC-based software.

Using a circular region of interest (ROI) of approximately 2 mm^2, the attenuation values (in Hounsfield unit; HU) of the common carotid artery and submandibular gland were measured in each of the 50 images. Care was taken to avoid the vessels in the parenchyma of submandibular gland within the ROI circle (Fig 1).

Time-attenuation curves were obtained in each scan and enhancement parameters were analyzed in the common carotid artery (A), submandibular gland (S). Enhancement parameters calculated for each images of scans included the peak enhancement (Imax), the time to peak enhancement (Tmax),

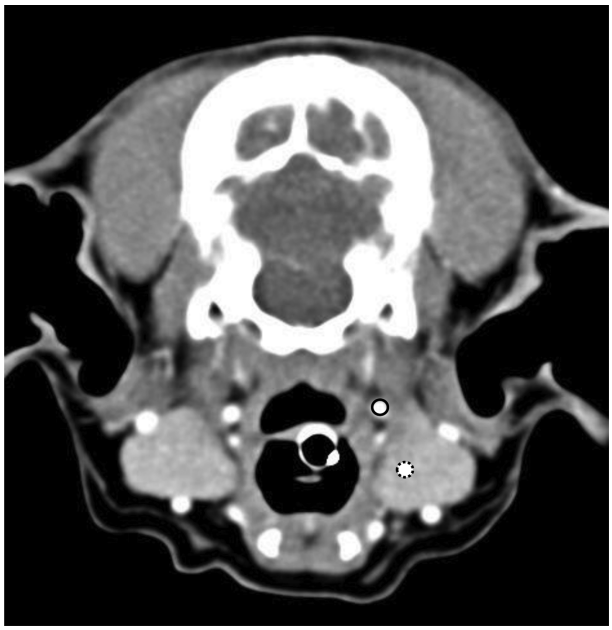

Fig 1. The region of interest (ROI) of the common carotid artery (black round), and submandibular gland (dotted round). Using a circular ROI of approximately 2 mm^2, Hounsfield Unit (HU) of the common carotid artery and submandibular gland were measured. Care was taken to avoid the vessels in the parenchyma of submandibular gland.

the time to equilibrium phase (Teq), and the time between peak enhancement in the common carotid artery and onset of the equilibrium phase (T-Aeq). The equilibrium phase proposed by Foley et al. represents the period where aortic and hepatic enhancement undergo gradual parallel decline (13). This definition was applied to the present study as the period where enhancement of common carotid artery and submandibular gland undergo gradual parallel decline.

Statistical analysis

Statistical tests were performed using commercially available statistical analysis software (SPSS25.0, SPSS Inc., Chicago, IL, USA). All data are expressed as means ± standard deviation for each group.

For the comparison of the effects of the postprandial times, differences in mean attenuation values between the 12H group and the remaining groups were analyzed for statistical significance by the use of one-way analysis of variance (ANOVA). When the differences were statistically significant, post hoc analysis was performed using Scheffe's multiple-comparison test. In the test, a P values less than 0.05 was considered to indicate a statistically significant difference.

Results

Representative enhancement parameters using dynamic CT in clinically normal beagle dogs

As preliminary experimentation, the mean enhancement parameters in normal beagle dogs whose fasting time was 12 hours were as follows: Imax of common carotid artery

(mean ± SD) was 472.49 ± 19.01 HU. Imax of the submandibular gland was 138.95 ± 6.25 HU. Tmax of common carotid artery and submandibular gland were 25.8 ± 1.79 sec and 69 ± 23.11 sec respectively. In Teq and T-Aeq, if these parameters could not be evaluated in 100 seconds of dynamic CT scanning, it was excluded from the analysis. Teq and T-Aeq (n = 4) was 80.5 ± 6.61 sec and 54.5 ± .51 sec respectively (Table 1).

Table 1. Representative enhancement parameters in normal beagle dogs whose fasting time was 12 hours

Parameters	Mean ± SD
ImaxA (HU)	472.49 ± 19.01
ImaxS (HU)	138.95 ± 6.25
TmaxA (sec)	25.8 ± 1.79
TmaxS (sec)	69 ± 23.11
Teq (sec)	80.5 ± 6.61 (n = 4)
T-Aeq (seq)	54.5 ± 5.51 (n = 4)

Imax (HU) of common carotid artery and submandibular gland in each group

The mean peak enhancement values of the common carotid artery (ImaxA) and submandibular gland (ImaxS) for each group is shown in Fig 2. In comparison with 12H group (12-hours fasting time), ImaxA and ImaxS in the 40M (40-minute fasting time) group were significantly higher than those in the 12H group ($p < 0.005$) respectively. There were significant differences between ImaxA of the 40M and 6H

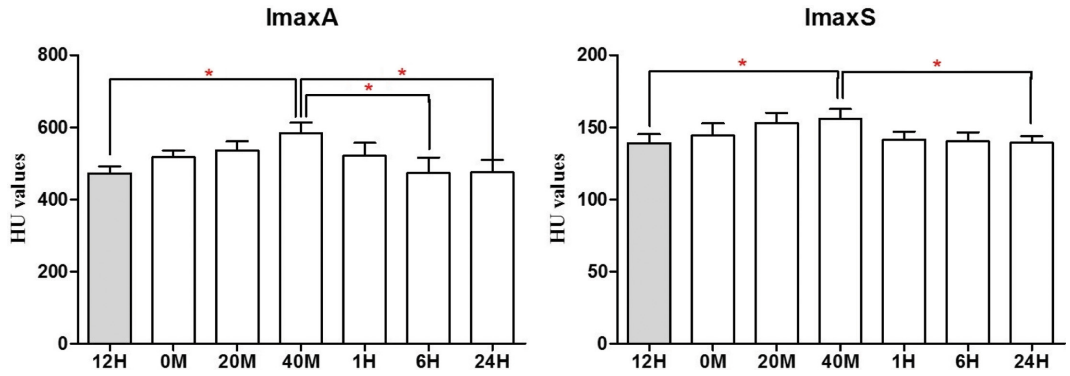

Fig 2. Imax (HU) of the common carotid artery and submandibular gland in each group. Graphs show peak enhancement value of common carotid artery (ImaxA) and submandibular gland (ImaxS) for each fasting time group. Significant differences between the groups are identified in the evaluation of the ImaxA and ImaxS (*; $p < 0.005$).

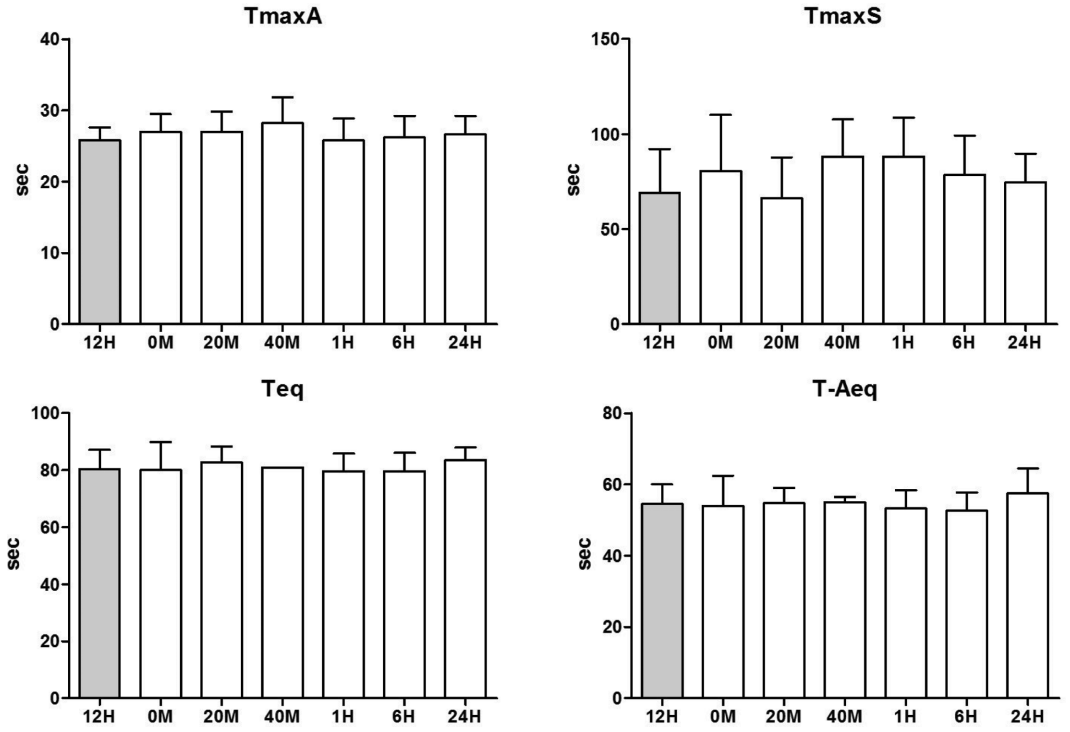

Fig 3. Tmax (sec) of common carotid artery and submandibular gland, Teq (sec) and T-Aeq (sec) in each group. Graphs show time to peak enhancement, Teq, and T-Aeq in fasting time groups. There are no statistically significant differences in the TmaxA, TmaxS, Teq and T-Aeq between fasting time groups.

group ($p < 0.005$) as well as in between those of the 40M and 24H group ($p < 0.005$). ImaxS in 24H group ($p < 0.005$) was also significantly different from the 40M group.

Tmax (sec) of common carotid artery and submandibular gland, Teq (sec) and T-Aeq (sec) in each group

There were no significant differences in the time to peak enhancement of the common carotid artery (TmaxA) and submandibular gland (TmaxS) between 12H and other groups. Additionally, no significant differences were observed in the Teq and T-Aeq (Fig 3).

Discussion

In human medicine, a few dynamic CT studies of submandibular glands were performed to optimize examination parameters for spiral CT scan (34,37). Moreover, it is reported that parametrical analysis of a contrast enhanced dynamic CT study can serve to differentiate the submandibular glandular diseases including salivary adenitis and salivary gland tumors (8,37,39). There were several protocols of dynamic CT examination in theses human studies. Enhancement parameters using the protocol (injected contrast material 50 ml with a flow of 1 ml/s) which the most similar to the present study were as follows: ImaxA – 127 ± 20 HU; ImaxS – 36 ± 7 HU; TmaxA – 45 ± 6 sec; TmaxS – 68 ± 34 sec (34). When comparing these parameters to results of the present study, ImaxA and ImaxS were lower and TmaxA was longer than results of the present study. TmaxS could not be compared due to the wide standard deviation. Contrast enhancement at CT is affected by various interacting factors. These factors can be divided into three categories: patient factors, contrast medium factors, and CT scanning factors. In case of patient factors, the major factors affecting contrast enhancement are body size and cardiac output (cardiovascular circulation time) (1). Therefore, the difference of enhancement parameters between human and dog may be due to the differences in body size, normal heart rate, and contrast medium volume.

In dogs, there were some protocols for contrast-enhanced CT images of liver and pancreas. Three-phase scanning for hepatic and pancreatic CT imaging was categorized as follows: arterial phase – 13 sec (liver) and 13 sec (pancreas); portal or venous phase – 30 sec (liver) and 28 sec (pancreas); equilibrium phase – 120 sec (liver) and 90 sec (pancreas) (15,18). In this study, the arterial phase and venous phase for submandibular gland were about 26 sec and 69 sec respectively and these were longer than those for liver and pancreas. The reason for this difference is not clear, however it may be explained by the differences in blood volume supplying to the organs and distance from injection site to the target organ (1). Difference in the equilibrium phase could not be evaluated because of the subjective evaluation of the time-attenuation curve pattern.

In author's experience, there were various degrees of contrast enhancement of salivary gland in patients without salivary gland diseases. Contrast enhancement in CT is affected by cardiovascular circulatory system such as cardiac output and cardiovascular circulation time (1). In previous study, by using Doppler ultrasonography in dogs, end diastolic velocity, mean velocity and blood flow volume increased significantly postprandially in the splanchnic vessels (29). In humans, likewise, these postprandial effects were also found in common carotid artery (11). Postprandial hemodynamic changes are known to result in increased blood flow volume and velocity in the splanchnic vessels such as cranial mesenteric artery and celiac artery. In dogs, it is known that these physiologic changes are significantly identified from 20 to 90 minutes postprandially (29). Similar hemodynamic changes are also observed between about 30 and 45 minutes postprandial in humans. Additionally, there were significant increases in common carotid artery flow volume and heart rate postprandially (10,11,19,24,25). External carotid artery is the main continuation of the common carotid artery and it has several branches. The facial artery, one of the external carotid branches, gives rise to glandular branch. This branch is the main supply to the mandibular salivary gland in dogs (4). Therefore, it can be suspected that the hemodynamic changes in the common carotid arteries can give effect to the contrast enhancement of salivary glands. In this study, significant increases in the ImaxA and ImaxS occurred after 40 minutes of food ingestion. These results were similar to those observed at the postprandial hemodynamic change in previous studies (11,29).

In previous studies, it is known that alteration of portal flow by means of food intake or hormonal administration can result in increased contrast enhancement of hepatic parenchyma. Administration of glucagon in dogs is known to cause a 23% increase in hepatic enhancement and decreased time to peak enhancement by a increase of portal blood flow (38). It is also reported that consuming a liquid meal increase hepatic enhancement by 11% in humans (17). These effects of hepatic enhancement may adversely affect hypervascular lesion conspicuity or improve detection of hypovascular lesion (17,32). In the present study, statistically significant increased enhancement of submandibular gland was identified after 40 minutes fasting. Thus, this may also have similar effects on the detection of lesions as the previous studies do. For minimizing this possibility, we recommend that the fasting time should be more than 12 hours.

The limitations of this study are as follows. First, the influences of factors associated with postprandial hemodynamic responses were not fully excluded. The stress factors (such as temperature and environment) stimulate the release of vasopressin from the hypophysis and lead to vasoconstriction of the splanchnic vessels (28). Gastric distension and the digestibility of the food have also effects on the postprandial mesenteric hyperemia (16,26,27). It is reported that the larger-volume and lower-fat meal increase the postprandial contrast enhancement (33). In this study, we did not control the amount and composition of the test meal. The second was that the present study was performed with only small number of clinically normal dogs. In this study, due to the small number of the dog, we just could obtain the normal enhancement parameters as preliminary study. Establishing reference range for the enhancement parameters with large number of dogs through further studies is needed for more accurate statistics. It is also necessary to differentiate between the normal and salivary glandular diseases.

Conclusion

In conclusion, as preliminary study, the enhancement parameters of dynamic CT for salivary gland in clinically normal dogs were as follows: ImaxA – 472.49 ± 19.01 HU; ImaxS – 138.95 ± 6.25 HU; TmaxA – 25.8 ± 1.79 sec; TmaxS – 69.0 ± 23.11 sec; Teq – 80.5 ± 6.61 sec; T-Aeq – 54.5 ± 5.51 sec. Additionally, due to postprandial hemodynamic changes, contrast enhancement of salivary gland was significantly increased in 40 minutes after eating. Because this result may have effects on the diagnosis of salivary glandular diseases, sufficient fasting time is important for accurate diagnosis.

References

1. Bae KT. Intravenous contrast medium administration and scan timing at CT: considerations and approaches. Radiology 2010; 256: 32-61.
2. Balthazar EJ, Robinson DL, Megibow AJ, Ranson JH. Acute pancreatitis: value of CT in establishing prognosis. Radiology 1990; 174: 331-336.
3. Baron RL, Oliver JH 3rd, Dodd GD 3rd, Nalensik M, Holbert BL, Carr B. Hepatocellular carcinoma: evaluation with biphasic, contrast-enhanced, helical CT. Radiology 1996; 199: 505-511.
4. Bezuidenhout A. The heart and Arteries. In: Miller's anatomy of the dog, 4th ed. St. Louis, Missouri: Elsevier. 2013: 444-447.
5. Bonaldi VM, Bret PM, Reinhold C, Atri M. Helical CT of the liver: value of and early hepatic arterial phase. Radiology 1995; 197: 357-363.
6. Boroffka S, Dennison S, Schwarz T, Saunders J. Orbita, Salivary glands and Lacrimal system. In: Veterinary Computed Tomography. Chichester, West Sussex: Wiley-Blackwell. 2011: 137-151.
7. Canon MS, Paglia D, Zwingenberger AL, Boroffka SA, Hollingsworth SR, Wisner ER. Clinical and diagnostic imaging findings in dogs with zygomatic sialadenitis: 11 cases (1990-2009). J Am Vet Med Assoc 2011; 239: 1211-1218.
8. Choi DS, Na DG, Byun HS, Ko YH, Kim CK, Cho JM, Lee HK. Salivary gland tumors: evaluation with two-phase helical CT Radiology 2000; 214: 231-236.
9. Chow FE, Stent AW, Milne M. Imaging diagnosis—Use of multiphasic contrast-enhanced computed tomography for diagnosis of mesenteric volvulus in a dog. Vet Radiol Ultrasound 2014; 55: 74-78.
10. Dalman RL, Li KC, Moon WK, Chen I, Zarins CK. Diminished postprandial hyperemia in patients with aortic and mesenteric arterial occlusive disease. Circulation 1996; 94: 206-210.
11. Eicke BM, Seidel E, Krummenauer F. Volume flow in the common carotid artery does not decrease postprandially. J Neuroimaging 2003; 13: 352-355.
12. Fife WD, Samii VF, Drost WT, Mattoon JS, Hoshaw-Woodard S. Comparison between malignant and nonmalignant splenic masses in dogs using contrast-enhanced computed tomography. Vet Radiol Ultrasound 2004; 45: 289-297.
13. Foley WD, Hoffmann RG, Quiroz FA, Kahn CE, Perret RS. Hepatic helical CT: Contrast material injection protocol. Radiology 1994; 192: 367-371.
14. Fossum TW. Preparation of the Operative Site. In: Small Animal Surgery, 4th ed. St. Louis, Missouri: Elsvier. 2013: 39.
15. Fukushima K, Kanemoto H, Ohno K, Takahashi M, Nakashima K, Fujino Y, Uchida K, Fujiwara R, Nishimura R, Tsujimoto H. CT characteristics of primary hepatic mass lesions in dogs. Vet Radiol Ultrasound 2012; 53: 252-257.
16. Gallavan RH Jr, Chou CC, Kvietys PR, Sit SP. Regional blood flow during digestion in the conscious dog. Am J Physiol 1980; 238: 220-225.
17. Irie T, Kusano S. Effects of a liquid meal on contrast-enhanced CT of the liver. Am J Roentgenol 1996; 167: 1023-1024.
18. Iseri T, Yamada K, Chijiwa K, Nishimura R, Matsunaga S, Fujisawara R, Sasaki N. Dynamic computed tomography of the pancreas in normal dogs and in a dog with pancreatic insulinoma. Vet Radiol Ultrasound 2007; 48: 328-331.
19. Kamata T, Yokota T, Furukawa T, Tsukagoshi H. Cerebral ischemic attack caused by postprandial hypotension. Stroke 1994; 25: 511-513.
20. Kim T, Murakami T, Takahasi S, Tsuda K, Tomoda K, Narumi Y, Oi H, Sakon M, Nakamura H. Optimal phases of dynamic CT for detecting hepatocellular carcinoma: evaluation of unenhanced and triple-phase images. Abdom Imaging 1999; 24: 473-480.
21. Lee NS, Choi MH, Keh SY, Kim TH, Kim HW, Yoon JH. Zygomatic sialolithiasis diagnosed with computed tomography in a dog. J Vet Med Sci 2014; 76: 1389-1391.
22. Lenoci D, Ricciardi M. Ultrasound and multidetector computed tomography of mandibular salivary gland adenocarcinoma in two dogs. Open Vet J 2015; 5: 173-178.
23. Lev MH, Khanduja K, Morris PP, Curtin HD. Parotid pleomorphic adenomas: delayed CT enhancement. Am J Neuroradiol 1998; 19: 1835-1839.
24. Levin LA, Mootha VV. Postprandial transient visual loss. A symptom of critical carotid stenosis. Ophthalmology 1997; 104: 397-401.
25. Parker DR, Carlisle K, Cowan RJ, Corrall RJ, Read AE. Postprandial mesenteric blood flow in humans: relationship to endogenous gastrointestinal hormone secretion and energy content of food. Eur J Gastroenterol Hepatol 1995; 7: 435-440.
26. Qamar MI, Read AE. Effects of ingestion of carbohydrate, fat, protein, and water on the mesenteric blood flow in man. Scand J Gastroenterol 1988; 23: 26-30.
27. Qamar MI, Read AE, Mountford R. Increased superior mesenteric artery blood flow after glucose but not lactulose ingestion. Q J Med 1986; 60: 893-836.
28. Rasmussen K. Non-invasive quantitative measurement of blood flow and estimation of vascular resistance by the Doppler ultrasound method. Dan Med Bull 1992; 39: 1-14.
29. Riesen S, Schmid V, Gaschen, L, Busato A, Lang J. Doppler measurement of splanchnic blood flow during digestion in unsedated normal dogs. Vet Radiol Ultrasound 2002; 43: 554-560.
30. Roberts HC, Roberts TP, Lee TY, Dillon WP. Dyanamic, contrast-enhanced CT of human brain tumors: quantitative assessment of blood volume, blood flow, and microvascular permeability: report of two cases. Am J Neuroradiol 2002; 23: 828-832.
31. Schultz RM, Wisner ER, Johnson EG, MacLeod JS. Contrast-enhanced computed tomography as a preoperative indicator of vascular invasion from adrenal masses in dogs. Vet Radiol Ultrasound 2009; 50: 625-629.
32. Sheafor DH, Keogan MT, DeLong DM, Nelson RC. Dynamic helical CT of the abdomen: prospective comparison of pre- and postprandial contrast enhancement. Radiology 1998; 206: 359-363.
33. Sidery MB, Macdonald IA, Blackshaw PE. Superior mesenteric artery blood flow and gastric emptying in humans and the differential effects of high fat and high carbohydrate meals.

Gut 1994; 35: 186-190.
34. Spreer J, Krahe T, Jung G, Lackner K. Spiral versus conventional CT in routine examinations of the neck. J Comput Assist Tomogr 1995; 19: 905-910.
35. Torad FA, Hassan EA. Clinical and ultrasonographic characteristics of salivary mucoceles in 13 dogs. Vet Radiol Ultrasound 2013; 54: 293-298.
36. Van Hoe L, Baert AL, Gryspeerdt S, Vandenbosh G, Nevens F, Van Steenbergen W, Marchal G. Dual-phase helical CT of the liver: value of an early-phase acquisition in the differential diagnosis of non-cystic focal lesions. Am J Roentgenol 1997; 168: 1185-1192.
37. Wakasa T, Higuchi Y, Hisatomi M, Aiga H, Honda Y, Kishi K. Application of Dynamic CT for various diseases in the oral and maxlliofacial region. Eur J Radiol 2002; 44: 10-15.
38. Warshauer DM, Hiken JN, Molina PL, Hackney SL, Bellinger DA, Lee JK. Hepatic contrast enhancement at CT: influence of intravenous glucagon in a canine model. Radiology 1995; 197: 365-368.
39. Yerli H, Aydin E, Coskun M, Geyik E, Ozluoglu LN, Haberal N, Kaskati T. Dynamic multislice computed tomography findings for parotid gland tumors. J Comput Assist Tomogr 2007; 31: 309-16.